THE JOURNAL OF PHYSICAL CHEMISTRY C

Review Article

pubs.acs.org/JPCC

Energies of Formation Reactions Measured for Adsorbates on Late Transition Metal Surfaces

Trent L. Silbaugh[†] and Charles T. Campbell*[,†,‡]

[†]Department of Chemical Engineering and [‡]Department of Chemistry, University of Washington, Seattle, Washington 98195-1700, United States

Supporting Information

ABSTRACT: The energies of adsorbates containing H, N, C, O, and halogens that are of interest as intermediates, poisons, and promoters in catalytic reactions have been measured on well-defined single-crystal surfaces by equilibrium adsorption isotherms, temperature-programmed desorption (TPD), and single-crystal adsorption calorimetry (SCAC). Here we tabulate a large collection of those experimental adsorption energies which we consider to be particularly reliable based on reproducibility by other groups, comparisons to results for closely related systems, and/or reliability of other results reported by the same group. Specifically, we list the enthalpies and energies of 81 molecular and dissociative adsorption reactions that were measured on 26 different metal single-crystal faces of 12 different late transition metals, and we extract from these the standard enthalpies of formation of the adsorbates thus produced. These can serve as benchmarks for validating computational methods for estimating surface reaction energies.

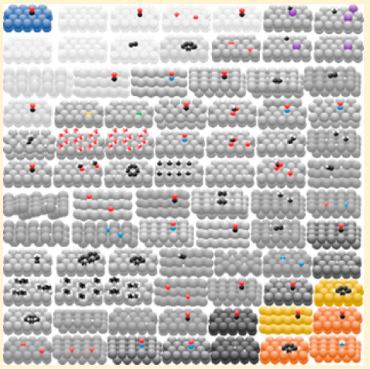

1. INTRODUCTION

Understanding the energetics of chemical reactions on late transition metal surfaces is crucial for the development and operations of many technologies that will be essential for our energy and environmental future. It would enable us to develop better catalysts for the production of clean fuels, for the combustion of fuels and the production of chemicals with improved energy efficiency and less pollution, and for environmental remediation. It would also help us to develop better fuel cells and batteries for improved energy efficiency and to design photocatalysts that can harvest the sun's energy. These are all essential ingredients for sustainable living with high quality of life. Here we summarize experimental measurements that markedly improve our understanding of the energetics of common adsorbed intermediates in energy-related and environmental catalysis on late transition metal surfaces. We present here a database of reliable energies of adsorbed catalytic intermediates that can be used as benchmarks to guide our understanding of the energetics of specific catalytic reactions and will help in the future development of improved computational methods for calculating the energetics (i.e., reaction energies and activation barriers) of elementary chemical reactions at late transition metal surfaces.

With the advent some 15 years ago of fast methods for doing density functional theory (DFT) calculations with periodic boundary conditions that were able to treat late transition metal surfaces with good energy accuracy,[1−4] surface chemistry research was revolutionized. The general feeling among the surface science community was that we finally had a method with predictive ability for surface chemistry. This resulted in an explosion in the number of studies utilizing DFT to investigate surface science problems. It is reasonable to estimate that at least 1000 groups worldwide now employ DFT to study problems in surface chemistry. This huge growth has been driven by the deep fundamental insights provided by DFT with periodic boundary conditions (which we will refer to as "periodic DFT" below) and also by the hope that it can accelerate the discovery of new materials where surface properties are crucial, such as catalytic and electrocatalytic materials. Indeed, the groups of Nørskov, Bligaard, Mavrikakis, Greeley, and others already have demonstrated some successes in using periodic DFT to guide the discovery of better catalytic materials.[5−17] It is clear that computational chemistry based on fast computational methods like periodic DFT will play a huge role in the future of research in heterogeneous catalysis and electrocatalysis.

However, we have recently shown that the energy accuracy of periodic DFT is still not sufficient for it to realize anywhere near its full potential for positively impacting catalysis research.[18] Specifically, the energy estimates of DFT using four common functionals were compared to a database of 39 reliable experimental measurements of adsorption reactions. Even the most accurate functional (BEEF-vdW), which incorporates van der Waals corrections, had a mean absolute error (MAE) of 16 kJ/mol, per molecular fragment produced, for "pure chemisorption" reactions that had little contribution from van der Waals interactions, compared to an average reaction energy of just −127 kJ/mol. For the reactions that had large van der Waals contributions to adsorbate bonding, the best MAE was larger (29 kJ/mol), over 43% of the average

Received: June 17, 2016
Revised: August 27, 2016
Published: September 14, 2016

DOI: 10.1021/acs.jpcc.6b06154
J. Phys. Chem. C 2016, 120, 25161−25172

reaction energy (−66 kJ/mol).[18] Nevertheless, the rapidly improving state of fast algorithms for computational quantum chemistry, combined with the rapidly accelerating speed and memory capacity of modern computers, will soon make it possible to do much more sophisticated computations at the same speed as today's periodic DFT. This holds great promise for markedly improving the energy accuracy of fast computational quantum chemistry for catalysis research. *However, accurate experimental measurements of adsorbate energies is essential to validate the energy accuracy of such new computational methods and guide their evolution.* Our earlier report presented a database of 39 such adsorption reaction energies.[18] Here, we extend that database to 81 energies, covering 26 different metal faces and 12 different late transition metals. A benchmarks database for energies of 10 adsorbates on Pt(111) has also recently been published along with DFT calculations by Gautier, Sautet, and co-workers.[19] Several systems reported there had been omitted in our previous database but are included here. The energetics for three entries from that small database differ from those reported here (Reaction #s: 54, 55, 77 in Table 1) for reasons explained in notes given at the end of Table S1 in the Supporting Information. The present tabulation consists of experimental measurements of adsorption reaction energies on late transition metals which were chosen for the high quality of the measurements and expected reliability of the reported values, keeping in mind the importance of accuracy when such experimental benchmarks are intended for use in improving theoretical methods. The criteria we used in choosing the values listed here include: (1) reproducibility by other groups, (2) comparisons to results for closely related systems, (3) quality of the experimental approach and reported data, and (4) reliability of other results reported by the same group.

EXPERIMENTAL METHODS

The experimental methods employed to collect the data compiled here are well established and have been described in great detail elsewhere. Here we will give brief descriptions of each technique. More detailed descriptions can be found in an earlier review[20] and in the papers cited below.

Temperature-programmed desorption (TPD) is used to measure the desorption rate of molecules adsorbed on well-defined single-crystal samples during a programmed (ideally linear) temperature ramp. Methodologies for the analysis of TPD data have been developed, with the simplest method for first-order desorption a Redhead analysis.[21] In such an analysis, a desorption prefactor of 10^{13} s^{-1} is often assumed. However, numerous studies over the years have shown that such an assumption can lead to large errors in calculated energetics. Indeed, a recent report by Campbell and Sellers[22] found that experimentally determined desorption prefactors were correlated with the gas-phase entropy of the adsorbate species. This correlation has shown that the assumption of a prefactor of 10^{13} s^{-1} can underestimate desorption prefactors by several orders of magnitude. Although more sophisticated TPD experiments with heating rate variation[23,24] or superior analysis methods, such as leading edge analysis[25] or line shape ("complete") analysis,[26] have been utilized to accurately and independently determine both prefactors and activation energies,[27] a large proportion of published work has reported desorption energetics based on a simple Redhead analysis with an assumed prefactor. We report here only TPD results where a prefactor was determined independently of activation energy or where an assumption of 10^{13} s^{-1} yields energetics in close agreement with other experimental techniques and is consistent with prefactor estimates using the method of Campbell and Sellers.[22] When such supporting studies with other methods besides TPD are not available, we have reanalyzed TPD data using improved prefactors estimated following Campbell and Sellers,[22] as for example for benzene on Cu, Ag, and Au surfaces below.

Equilibrium methods for determining isosteric heats of adsorption of molecules on solid surfaces have been used since the early days of surface science research, born out of the pioneering work of Irving Langmuir.[28] Isosteric energetics have been determined from adsorption isotherms or isobars, whereby the gas partial pressure or sample temperature are varied while holding other variables constant and using changes in sample work function or changes in low energy electron diffraction peak intensities to monitor relative surface coverages of adsorbates. Such methods have been successfully employed to accurately determine adsorption energetics.[29,30]

Modulated molecular beam studies have also been utilized to obtain accurate adsorption energetics,[31−34] with time-dependent detection of scattered molecules being carried out with techniques such as quadrupole mass spectrometry or temperature-resolved electron energy loss spectroscopy (TREELS).

All of the above-mentioned experimental techniques suffer from the drawback that desorption must be a reversible process. This limitation had precluded the study of many molecules, particularly those of interest in the catalysis field, that react upon adsorption to form interesting intermediates, as such processes are rarely reversible. The pioneering development of the technique of single-crystal adsorption calorimetry (SCAC) by Sir David King and co-workers was carried out in direct response to these limitations. Following further refinement in detection methods by Campbell and co-workers, this technique has been used by several groups to study irreversible adsorption systems and to report on the energetics of many catalytically relevant adsorbed intermediates. Several reviews and compilations of reported work have been published on SCAC.[35−37]

RESULTS AND DISCUSSION

Table 1 lists the standard reaction enthalpies for the full set of adsorption reactions analyzed here, the measurement temperatures and coverages, the measurement method, and the citations whose enthalpies were included in the average value reported here. These are the enthalpy changes for the reaction *per mole as written,* integrated (i.e., averaged) from zero coverage of the reacted gas up to its listed coverage (removing, where possible, contributions from defect sites). "Standard" here simply means at 1 bar pressure (using the ideal gas law to correct the PV term in enthalpies to 1 bar via $PV/n = RT$). The coverages listed here are defined as the number of reacted gas molecules in the reaction as written per metal surface atom, with the exception of diatomic molecules that dissociatively adsorb (H_2, N_2, O_2), where coverage is defined as the number of adsorbed atomic species per metal surface atom. We list integral heats of adsorption rather than differential heats here since they more readily compare to periodic DFT calculations, which give integral energies of adsorption. We use a coverage of 1/4 ML when data were available since such calculations are less expensive at this high coverage and thus are more commonly found in the literature. For large molecules which cannot achieve high coverages, such as benzene, a coverage of 1/9 ML was chosen to allow for comparison to periodic DFT with a reasonably small unit cell. As noted in the footnotes to

DOI: 10.1021/acs.jpcc.6b06154
J. Phys. Chem. C 2016, 120, 25161−25172

Table 1. Experimental Reaction Enthalpies and Reaction Energies at the Listed Temperature and Surface Coverage and at 1 Bar Pressure of Pure Gas for Each Gas, Obtained by Averaging the Results from the Listed References as Listed in Table S1[a]

#	surface reaction	coverage (ML)[d]	reaction enthalpy (kJ/mol)[e]	temp (K)	reaction energy (kJ/mol)	exptl method[f]	refs	comments
1	CO + Ni(111) → CO/Ni(111)	1/4	−122	353	−119	SCAC, EQBM, TPD	35,48−50	
		<0.1	−130	300	−128	SCAC	35	
		<0.015	−130	420	−127	TPD	51	
2	CO + Ni(110) → CO/Ni(110)	1/4	−128	380	−126	SCAC, TPD, EQBM	35,52−54	$A = \sim 10^{15}$ s^{-1}
3	CO + Ni(100) → CO/Ni(100)	1/4	−126	340	−124	SCAC	35,55−58	$A = 6 \times 10^{15}$ s^{-1}. C on surf. after TPD sequence
4	CO + Pt(111) → CO/Pt(111)	1/4	−120	344	−117	SCAC, TPD, EQBM	35[b],38,59−62	$A = 2 \times 10^{14}$ s^{-1}
5	CO + Pt(110) → CO/Pt(110)	1/4	−140	447	−137	SCAC, TPD, EQBM, MBRS	35[b],63,64	may be lifting of surface reconstruction on SCAC time scale. $A = 6 \times 10^{14}$ s^{-1}
6	CO + Pt(100)-hex → CO/Pt(100)-hex	1/2	−126	300	−124	SCAC	35,65[b]	
7	CO + Pt(100)-(1 × 1) → CO/Pt(100)-(1 × 1)	1/2	−141	300	−139	SCAC	35,65[b]	
8	CO + Pd(111) → CO/Pd(111)	1/4	−143	498	−139	TPD, EQBM, MMB	30,31,66−71	
9	CO + Pd(100) → CO/Pd(100)	1/4	−155	492	−151	EQBM	29,72,73	
10	CO + Rh(111) → CO/Rh(111)	1/4	−139	477	−135	MMB-TREELS, TPD, EQBM	74−76	
11	CO + Ir(111) → CO/Ir(111)	1/4	−158	420	−155	TPD	77	
12	CO + Cu(111)→ CO/Cu(111)	1/4	−53	150	−52	EQBM	78,79	
13	CO + Ru(0001) → CO/Ru(0001)	1/4	−158	475	−154	EQBM and TPD	80,81	
14	CO + Co(0001) → CO/Co(0001)	1/4	−115	370	−112	TPD	82	
15	CO + Ag(111) → CO/Ag(111)	1/4	−23	100	−22	EQBM	83	
16	CO + Ag(110) → CO/Ag(110)	lim 0 cov	−23	77	−21	EQBM, MMB	33,34	$A = 10^{(14.6\pm0.8)}$ s^{-1}, $A = 10^{(13.6\pm0.9)}$ s^{-1}
17	CO + Au(110)-(1 × 2) → CO/Au(110)-(1 × 2)	1/4	−49	160	−48	EQBM	84	
18	NO + Ni(100) → N/Ni(100) + O/Ni(100)	1/8	−290	300	−288	SCAC	35	
19	NO + Pt(111) → NO/Pt(111)	1/4	−114	300	−112	SCAC	85[b]	
20	NO + Pt(110) → NO/Pt(110)	1/4	−113	300	−111	SCAC	86[b]	
21	NO + Pt(100)-hex → NO/Pt(110)-hex	1/4	−116	300	−114	SCAC	35	
22	NO + Pt(100)-(1 × 1) → NO/Pt(110)-(1 × 1)	1/4	−120	300	−118	SCAC	35	
23	NO + Pt(211) → NO/Pt(211)	1/4	−128	300	−126	SCAC	85[b]	initially dissociative adsorption
24	NO + Pd(111) → NO/Pd(111)	1/4	−179	520	−175	TPD	87	
25	NO + Pd(100) → NO/Pd(100)	1/4	−161	300	−159	SCAC	35[b]	
26	O_2 + Ni(111) → 2 O/Ni(111)	1/4	−480	300	−476	SCAC	35	
27	O_2 + Ni(110) → 2 O/Ni(110)	1/4	−470	300	−466	SCAC	35	surface reconstruction
28	O_2 + Ni(100) → 2 O/Ni(100)	1/4	−530	300	−528	SCAC	35,88	
29	O_2 + Pt(111) → 2 O/Pt(111)	1/9	−208	515	−204	SCAC, TPD	85[b],39,89,90	
30	O_2 + Pt(110) → 2 O/Pt(110)	1/4	−220	300	−216	SCAC	86[b]	
31	O_2 + Rh(100) → 2 O/Rh(100)	1/4	−358	300	−356	SCAC	35,88	
32	N_2 + Fe(100) → 2 N/Fe(100)	1/2	−220	950	−212	TPD, N_2 Uptake	91	
33	N_2 + Ni(111) → 2 N/Ni(111)	1/12	−109	440	−107	TPD	92	surface reconstruction[93]

J. Phys. Chem. C 2016, 120, 25161−25172
DOI: 10.1021/acs.jpcc.6b06154

Table 1. continued

#	surface reaction	coverage (ML)[d]	reaction enthalpy (kJ/mol)[e]	temp (K)	reaction energy (kJ/mol)	exptl method[f]	refs	comments
34	H_2 + Pt(111) → 2H/Pt(111)	1/4	−72	225	−70	TPD, EQBM, MMB	94,95	
35	H_2 + Ni(111) → 2H/Ni(111)	1/4	−94	370	−91	EQBM	46,96	
36	H_2 + Ni(100) → 2H/Ni(100)	1/4	−94	370	−91	EQBM	46,96	
37	H_2 + Fe(111) → 2H/Fe(111)	1/4	−88	370	−85	TPD	97	
38	H_2 + Fe(110) → 2H/Fe(110)	1/4	−110	450	−106	TPD	97	
39	H_2 + Fe(100) → 2H/Fe(100)	1/9	−81	420	−78	TPD	97	
40	H_2 + Rh(111) → 2H/Rh(111)	1/4	−70	325	−67	TPD	98	
41	H_2 + Pd(111) → 2H/Pd(111)	1/4	−88	370	−85	TPD	46,96	
42	D_2 + Ir(111) → 2D/Ir(111)	1/4	−60	310	−57	TPD	99	$A = 10^{-5}$ cm^2/s decreasing reaction enthalpy between 0 and 1/8 ML, constant above 1/8 ML
43	H_2 + Ru(0001) → 2H/Ru(0001)	1/4	−116	390	−113	TPD	100	$A = 2 \times 10^{14}$ s^{-1}
44	H_2 + W(100) → 2H/W(100)	1/4	−172	450	−168	EQBM	101	$A = 5 \times 10^3$ cm^2/s ($\sqrt{2} \times \sqrt{2}$) surf. reconstruction
45	I + Pt(111) → I/Pt(111)	1/3	−222	0	−222	TPD	102	
		1/4	−230	0	−230	TPD	102	
		1/8	−243	0	−243	TPD	102	
		0.07	−248	0	−248	TPD	102	
46	Cl + Pt(111) → Cl/Pt(111)	∼1/8	−238	880	−231	TPD	103	
47	F + Pt(111) → F/Pt(111)	0.07	−252	920	−244	TPD	104	
48	NH_3 + Cu(100) → NH_3/Cu(100)	1/4	−57	235	−55	MMB- TREELS	32	$A = 10^{(13.4\pm0.4)}$ s^{-1}
49	CH_3I + Pt(111) → CH_3I/Pt(111)	1/4	−83[h]	100	−82	SCAC	105	
50	CH_3OH + Pt(111) → CH_3OH/Pt(111)	1/9	−57[h]	100	−56	SCAC	106	
		1/4	−58[h]	100	−55	SCAC	106	
51	D_2O + Pt(111) → D_2O/Pt(111)	∼2/3	−51	120	−50	SCAC	40	hexagonal network, big islands
52	HCOOH + Pt(111) → HCOOH/Pt(111)	1/4	−58[h]	100	−57	SCAC	107	
53	CH_4 + Pt(111) → CH_4/Pt(111)	1/2	−15	63	−15	TPD[g]	108	methane
54	C_2H_6 + Pt(111) → C_2H_6/Pt(111)	1/3	−29	106	−28	TPD[g]	108	ethane
55	C_3H_8 + Pt(111) → C_3H_8/Pt(111)	1/4	−41	139	−40	TPD[g]	108	propane
56	C_4H_{10} + Pt(111) → C_4H_{10}/Pt(111)	1/3	−51	171	−49	TPD[g]	108	*n*-butane
57	c-C_6H_6 + Pt(111) → c-C_6H_6/Pt(111)	1/9	−164	300	−162	SCAC	59,109	benzene
58	c-C_6H_6 + Cu(111) → c-C_6H_6/Cu(111)	1/9	−68	225	−66	TPD	110,111[c]	benzene
59	c-C_6H_6 + Ag(111) → c-C_6H_6/Ag(111)	1/9	−63	210	−61	TPD	112[c]	benzene
60	c-C_6H_6 + Au(111) → c-C_6H_6/Au(111)	1/9	−72	230	−70	TPD	113[c]	benzene
61	c-C_6H_{10} + Pt(111) → c-C_6H_{10}/Pt(111)	1/9	−120[h]	100	−119	SCAC	95	cyclohexene
62	$C_{10}H_8$ + Pt(111) → $C_{10}H_8$/Pt(111)	1/16	−265	300	−263	SCAC	114	naphthalene
63	CH_3OH + O/Pt(111) → CH_3O/Pt(111) + OH/Pt(111)	1/4	−74[h]	150	−73	SCAC	106	
64	CH_3I + Pt(111) → CH_3/Pt(111) + I/Pt(111)	1/25	−210[h]	320	−207	SCAC	115	
65	CH_2I_2 + Pt(111) → CH/Pt(111) + H/Pt(111) + 2I/Pt(111)	1/12	−470[h]	210	−468	SCAC	116	
66	D_2O + 1/3O/Pt(111) → 2/3(D_2O···OD)/Pt(111)	1/2	−57	150	−56	SCAC	41	
67	HCOOH + O/Pt(111) → $HCOO_{mon}$/Pt(111) + OH/Pt(111)	1/4	−78[h]	130	−77	SCAC	107	monodentate formate

J. Phys. Chem. C 2016, 120, 25161−25172 DOI: 10.1021/acs.jpcc.6b06154

Table 1. continued

#	surface reaction	coverage (ML)[d]	reaction enthalpy (kJ/mol)[e]	temp (K)	reaction energy (kJ/mol)	exptl method[f]	refs	comments
68	HCOOH + O/Pt(111) → $HCOO_{bi}$/Pt(111) + OH/Pt(111)	1/4	−113[h]	170	−112	SCAC	107	bidentate formate
69	C_2H_4 + Ni(100) → 2≡CH/Ni(100) + 2H/Ni(100)	Init.	−203	300	−201	SCAC	35	
70	C_2H_4 + Ni(100) → −CCH/Ni(100) + 3H/Ni(100)	0.07	−140	300	−138	SCAC	35	σ and π bonding
71	C_2H_4 + Ni(110) → −CCH/Ni(110) + H/Ni(110)	Init.	−120	300	−118	SCAC	35	σ and π bonding
72	C_2H_2 + Ni(100) → 2≡CH/Ni(100)	Init.	−265	300	−263	SCAC	35	
73	C_2H_2 + Ni(100) → −CCH/Ni(100) + H/Ni(100)	1/4	−150	300	−148	SCAC	35	σ and π bonding
74	C_2H_2 + Ni(110) → −CCH/Ni(110) + H/Ni(110)	Init.	−180	300	−178	SCAC	35	
75	C_2H_2 + Rh(100) → −CCH/Rh(100) + H/Rh(100)	Init.	−175	300	−173	SCAC	35	
76	C_2H_4 + Pt(111) → =CH−CH_3/Pt(111) + H/Pt(111)	Init.	−138	300	−136	SCAC	35[b]	
77	C_2H_4 + Pt(111) → ≡C−CH_3/Pt(111) + 1/2H_2	1/6	−99	300	−97	SCAC	35[b]	
78	C_2H_4 + Pt(100)-hex → =CH−CH=/Pt(100)-hex + 2H/Pt(100)-hex	Init.	−150	300	−148	SCAC	35[b]	
79	C_2H_4 + Pt(100)-(1 × 1) → =CH−CH=/Pt(100)-(1 × 1) + 2H/Pt(100)-(1 × 1)	Init.	−215	300	−213	SCAC	35[b]	
80	C_2H_4 + Pt(100)-(1 × 1) → −CH=CH−/Pt(100)-(1 × 1) + 2H/Pt(100)-(1 × 1)	1/3	−106	300	−104	SCAC	35[b]	
81	c-C_6H_{10} + Pt(111) → c-C_6H_9/Pt(111) + H/Pt(111)	0.12	−132[h]	281	−130	SCAC	95	π-allyl c-C_6H_9

[a]Experimental technique acronyms are defined below the table. For specific reference information, see Table S1 where entries for each reference are provided. Desorption prefactors listed under Comments are taken from individual references (see Table S1). [b]This entry was corrected from the original value reported as described in refs 18 and 39. [c]This entry was corrected using an improved prefactor calculated from gas-phase entropies based on the method outlined by Campbell and Sellers.[22] [d]These coverages are defined here as the number of reacted gas molecules in the reaction *as written* per metal surface atom, with the exception of reactions 26−44 where coverage refers to the number of adsorbed atoms per metal surface atom. [e]These are the enthalpy changes for the reaction per mole of reacted gas *as written*, integrated from zero coverage of the reacted gas up to its listed coverage. When necessary, enthalpy changes reported here are obtained from Arrhenius desorption barriers by subtracting 1/2*RT* from the positive barrier values and changing sign. The enthalpy changes are converted to changes in internal energy by adding the small correction of + *RT* (= +2.5 kJ/mol at 300 K). Assuming ideal gas behavior up to 1 bar, these thus correspond to all the gas-phase reactants and products at 1 bar pressure of pure gas for each gas listed in the reaction, and thus its "standard state". [f]The acronyms used in this column refer to the following experimental techniques: single-crystal adsorption calorimetry (SCAC), temperature-programmed desorption (TPD), equilibrium measurements of coverage versus temperature and pressure (EQBM), modulated molecular beam measurements of surface residence times versus temperature (MMB), time-resolved electron energy loss spectroscopy (TREELS), equilibrium measurements using laser-induced thermal desorption (EQBM-LITD). [g]These coverages refer to the packing density in the islands of these adsorbates and refer to a situation where half the surface was covered by the nearly close-packed islands (but the enthalpy changed very little with this fraction, due to this islanding). [h]These entries were decreased in absolute magnitude by 2−3 kJ/mol from original publications, to correct a systematic error equal to RT_{source}, where T_{source} is the temperature of the molecular beam source (298−350 K). This arose due to a typographical error in ref 95, where a negative sign is missing in eqs (5) and (8) on "1/2 RT_{source}".

J. Phys. Chem. C 2016, 120, 25161−25172 DOI: 10.1021/acs.jpcc.6b06154

Table 1, the coverages of certain adsorbate systems were chosen based on the coverage of the specific surface structure that was produced experimentally (usually in islands).

Enthalpy changes reported here that were determined from Arrhenius activation energies for desorption were obtained by adding 1/2 RT to the positive activation energy reported and changing sign.[35] All enthalpy changes here can be converted to changes in internal energy by adding the small correction (per mole of reacted gas) of $+RT$ (= +2.5 kJ/mol at 300 K). Caution should be exercised in comparing these internal energy changes to quantum mechanical calculations at T = 0 K, since the temperature-integrated heat capacity must be considered, and that can sometimes be substantial.

The acronyms used in this table refer to the following experimental techniques: single-crystal adsorption calorimetry (SCAC), temperature-programmed desorption (TPD), equilibrium measurements of coverage versus temperature and pressure (EQBM), modulated molecular beam measurements of surface residence times versus temperature (MMB), and time-resolved electron energy loss spectroscopy (TREELS). The enthalpies and energies in Table 1 are the averages of the values reported in the papers cited there. The values from the individual publications which were averaged are listed in Table S1. Our previous publication[18] included the energies for a subset of 39 of the 81 systems tabulated here (Reaction #s 1, 4, 8−14, 18, 19, 24−26, 28, 29, 31, 34−36, 40, 41, 45, 48−51, 53−61, 64−66), with identical values except for Reaction #s 49, 61, 64, and 65, which contained a small systematic error (see Table 1 footnote).

Earlier papers[18,38,39] have described in detail the need for the recalibration of SCAC energetics reported in the review by Brown et al.,[35] due to the use of incorrect optical reflectivities of the samples in the calorimeter's calibration. SCAC data reported in that review reanalyzed raw data from many earlier reports from the same group to account for analysis errors and were therefore used in place of the primary references therein.[35] The energetics reported in Table S1 and denoted by * references have been corrected for this calibration error using correction factors of 0.71 for all Pt surfaces and 1.19 for Pd(100), based on values reported earlier.[18,38,39] Temperature-programmed desorption data for benzene on Cu(111), Au(111), and Ag(111) were reanalyzed here using a better estimate of the prefactor for desorption than that originally assumed, using instead $10^{15.6}$ s^{-1} following a report by Campbell and Sellers.[22] When reporting heats based on TPD data, we have chosen only systems where adsorption barriers are known to be less than 3 kJ/mol (and in most cases much closer to 0 kJ/mol).

For some adsorbate systems listed in Table 1, adsorbate−adsorbate interactions lead to the formation of ordered structures that are present in islands below saturation coverages, so we list their coverages in Table 1 as the local coverage within these islands. For example, islands of D_2O hexagonal networks[40] and the $(\sqrt{3} \times \sqrt{3})$R30 phase of $(D_2O{-}OD)$[41] are well established. The formation of hydrogen-bonded networks of adsorbed formic acid[42] and methanol[43,44] have also been reported. Based on island structures of saturated linear alkanes adsorbed on Pt(111) extrapolated from the island structure of octane on Pt(111),[45] C_nH_{2n+2} adsorbates create islands where individual molecules within this island structure occupy n + 1 surface metal atoms (unit cells of the metal surface).

Adsorbate-induced surface reconstruction is also a well-documented phenomenon, with the H/W(100) system being a classic example of such behavior.[46] In the case of the Pt(100) surface, SCAC measurements were able to differentiate adsorption energies on both the -(1 × 1) and −hex surfaces and, from these data, were able to determine quantitatively the thermodynamic driving force for adsorbate-induced reconstruction on this surface.[47] Although the corrections applied to this data, as discussed above, change the absolute values, the overall conclusions made in that paper still hold for CO-induced reconstruction of Pt(100). All entries in Table 1 and Table S1 where surface reconstruction is known to occur upon adsorption are identified as such in the Comments column. Great care should be taken when using such systems to compare to theoretical calculations, as the surface structure obtained upon reconstruction may be coverage dependent.

Adsorption energies based on TPD were recently reported for benzene on Cu, Ag, and Au(111).[117] We do not include those values here because: (1) actual TPD data for Cu and Au were not presented, (2) values for Cu and Au were reported only for the zero-coverage limit, which is where defect sites have the largest effects, (3) the pre-exponential factors were not reported and those values are important as a validation check, (4) the discrepancy of the Au(111) result with earlier literature[113] was not discussed, and (5) for the Ag(111) system, the coverage of 0.1 ML stated in the main text is inconsistent with the range reported in the Supporting Information of that same paper.

Since measurement errors were not reported in many of the cited studies, it is important to briefly discuss expected measurement errors for the various techniques included here, with the caveat that these are estimated errors and should not be applied to individual values. Errors in activation barriers determined from TPD experiments are typically within 5% but may be larger if the thermocouple was not attached properly. (For the data included here, we verified that the TPD peak temperatures agreed with those from other papers when available.) Selected equilibrium, MMB, and MMB-TREELS experiments included herein have reported measurement errors of ±1.2 kJ/mol (CO on Ag(110)[33]), ±1.5 kJ/mol (CO on Ag(110)[34]), and ±1.7 kJ/mol (NH_3 on Cu(100)[32]), respectively. Heats of reaction from SCAC experiments are within 3%. While these reported measurement errors can be instructive in assessing the accuracy within a single set of experiments, systematic errors present in the measurements can only be assessed through comparison across multiple studies using different experimental techniques. There are a limited number of systems where enough reliable data are available to comment on systematic errors in measurements. For example, the average enthalpy of adsorption of CO on Pt(111) reported here has a standard deviation of 1.8 kJ/mol based on 5 measurements from 3 different experimental techniques. A similarly low standard deviation (1.7 kJ/mol) is obtained for CO adsorption on Ni(111) based on 4 measurements using 3 different experimental techniques. However, much larger standard deviations of 6.1 and 6.4 kJ/mol are obtained for CO adsorption on Ni(100) (4 measurements using 3 techniques) and Pd(111) (8 measurements using 3 techniques), respectively. It is therefore difficult and potentially misleading to apply an estimate of the measurement error for a given experimental technique to systems contained herein that have fewer measurements and no reported errors, as systematic errors may be larger than reported measurement errors. Based

DOI: 10.1021/acs.jpcc.6b06154
J. Phys. Chem. C 2016, 120, 25161−25172

Table 2. Standard Enthalpies of Formation of Adsorbed Species at Standard Pressure (1 bar) and Listed Temperature, Calculated by Adding the Standard Enthalpy of the Corresponding Reaction Listed in Table 1 (at the Same #) to the Standard Enthalpy of Formation of Reactants *at the Listed Temperature* and Subtracting the Standard Enthalpies of Formation of Coadsorbates (Also Corrected to Reaction Temperature)[a]

#	surface reaction	coverage (ML)[d]	reaction enthalpy (kJ/mol)[e]	temp. (K)	enthalpy of formation of first listed adsorbate[a,b,c] (kJ/mol)
1	CO + Ni(111) → CO/Ni(111)	1/4	−122	353	−232
		<0.1	−130	300	−241
		<0.015	−130	420	−240
2	CO + Ni(110) → CO/Ni(110)	1/4	−128	380	−238
3	CO + Ni(100) → CO/Ni(100)	1/4	−126	340	−236
4	CO + Pt(111) → CO/Pt(111)	1/4	−120	344	−230
5	CO + Pt(110) → CO/Pt(110)	1/4	−140	447	−250
6	CO + Pt(100)-hex → CO/Pt(100)-hex	1/2	−126	300	−237
7	CO + Pt(100)-(1 × 1) → CO/Pt(100)-(1 × 1)	1/2	−141	300	−252
8	CO + Pd(111) → CO/Pd(111)	1/4	−143	498	−253
9	CO + Pd(100) → CO/Pd(100)	1/4	−155	492	−265
10	CO + Rh(111) → CO/Rh(111)	1/4	−139	477	−249
11	CO + Ir(111) → CO/Ir(111)	1/4	−158	420	−268
12	CO + Cu(111)→ CO/Cu(111)	1/4	−53	150	−165
13	CO + Ru(0001) → CO/Ru(0001)	1/4	−158	475	−268
14	CO + Co(0001) → CO/Co(0001)	1/4	−115	370	−225
15	CO + Ag(111) → CO/Ag(111)	1/4	−23	100	−136
16	CO + Ag(110) → CO/Ag(110)	lim 0 cov	−23	77	−136
17	CO + Au(110)-(1 × 2) → CO/Au(110)-(1 × 2)	1/4	−49	160	−161
18	NO + Ni(100) → N/Ni(100) + O/Ni(100)	1/8	−290	300	−200
19	NO + Pt(111) → NO/Pt(111)	1/4	−114	300	−24
20	NO + Pt(110) → NO/Pt(110)	1/4	−113	300	−23
21	NO + Pt(100)-hex → NO/Pt(110)-hex	1/4	−116	300	−26
22	NO + Pt(100)-(1 × 1) → NO/Pt(110)-(1 × 1)	1/4	−120	300	−30
23	NO + Pt(211) → NO/Pt(211)	1/4	−128	300	−38
24	NO + Pd(111) → NO/Pd(111)	1/4	−179	520	−89
25	NO + Pd(100) → NO/Pd(100)	1/4	−161	300	−71
26	O_2 + Ni(111) → 2O/Ni(111)	1/4	−480	300	−480
27	O_2 + Ni(110) → 2O/Ni(110)	1/4	−470	300	−470
28	O_2 + Ni(100) → 2O/Ni(100)	1/4	−530	300	−530
29	O_2 + Pt(111) → 2O/Pt(111)	1/9	−208	515	−208
30	O_2 + Pt(110) → 2O/Pt(110)	1/4	−220	300	−220
31	O_2 + Rh(100) → 2O/Rh(100)	1/4	−358	300	−358
32	N_2 + Fe(100) → 2N/Fe(100)	1/2	−220	950	−220
33	N_2 + Ni(111) → 2N/Ni(111)	1/12	−109	440	−109
34	H_2 + Pt(111) → 2H/Pt(111)	1/4	−72	300	−72
35	H_2 + Ni(111) → 2H/Ni(111)	1/4	−94	370	−94
36	H_2 + Ni(100) → 2H/Ni(100)	1/4	−94	370	−94
37	H_2 + Fe(111) → 2H/Fe(111)	1/4	−88	370	−88
38	H_2 + Fe(110) → 2H/Fe(110)	1/4	−110	450	−110
39	H_2 + Fe(100) → 2H/Fe(100)	1/9	−81	420	−81
40	H_2 + Rh(111) → 2H/Rh(111)	1/4	−70	325	−70
41	H_2 + Pd(111) → 2H/Pd(111)	1/4	−88	370	−88
42	D_2 + Ir(111) → 2D/Ir(111)	1/4	−60	310	−60
43	H_2 + Ru(0001) → 2H/Ru(0001)	1/4	−116	390	−116
44	H_2 + W(100) → 2H/W(100)	1/4	−172	450	−172
45	I + Pt(111) → I/Pt(111)	1/3	−222	0	−114
		1/4	−230	0	−122
		1/8	−243	0	−135
		0.07	−248	0	−140
46	Cl + Pt(111) → Cl/Pt(111)	∼1/8	−238	880	−114
47	F + Pt(111) → F/Pt(111)	0.07	−252	920	−170
48	NH_3 + Cu(100) → NH_3/Cu(100)	1/4	−57	235	−102
49	CH_3I + Pt(111) → CH_3I/Pt(111)	1/4	−83[f]	100	−61
50	CH_3OH + Pt(111) → CH_3OH/Pt(111)	1/9	−57[f]	100	−248
		1/4	−56[f]	100	−247
51	D_2O + Pt(111) → D_2O/Pt(111)	∼2/3	−51	120	−299

DOI: 10.1021/acs.jpcc.6b06154
J. Phys. Chem. C 2016, 120, 25161−25172

Table 2. continued

#	surface reaction	coverage (ML)[d]	reaction enthalpy (kJ/mol)[e]	temp. (K)	enthalpy of formation of first listed adsorbate[a,b,c] (kJ/mol)
52	$HCOOH + Pt(111) \rightarrow HCOOH/Pt(111)$	1/4	−58[f]	100	−432
53	$CH_4 + Pt(111) \rightarrow CH_4/Pt(111)$	1/2	−15	63	−85
54	$C_2H_6 + Pt(111) \rightarrow C_2H_6/Pt(111)$	1/3	−29	106	−103
55	$C_3H_8 + Pt(111) \rightarrow C_3H_8/Pt(111)$	1/4	−41	139	−135
56	$C_4H_{10} + Pt(111) \rightarrow C_4H_{10}/Pt(111)$	1/3	−51	171	−166
57	$c\text{-}C_6H_6 + Pt(111) \rightarrow c\text{-}C_6H_6/Pt(111)$	1/9	−164	300	−81
58	$c\text{-}C_6H_6 + Cu(111) \rightarrow c\text{-}C_6H_6/Cu(111)$	1/9	−68	225	19
59	$c\text{-}C_6H_6 + Ag(111) \rightarrow c\text{-}C_6H_6/Ag(111)$	1/9	−63	210	25
60	$c\text{-}C_6H_6 + Au(111) \rightarrow c\text{-}C_6H_6/Au(111)$	1/9	−72	230	15
61	$c\text{-}C_6H_{10} + Pt(111) \rightarrow c\text{-}C_6H_{10}/Pt(111)$	1/9	−120[f]	100	−18
62	$C_{10}H_8 + Pt(111) \rightarrow C_{10}H_8/Pt(111)$	1/16	−265	300	−182
63	$CH_3OH + O/Pt(111) \rightarrow CH_3O/Pt(111) + OH/Pt(111)$	1/4	−74[f]	150	−159
64	$CH_3I + Pt(111) \rightarrow CH_3/Pt(111) + I/Pt(111)$	1/25	−210[f]	320	−51
65	$CH_2I_2 + Pt(111) \rightarrow CH/Pt(111) + H/Pt(111) + 2I/Pt(111)$	1/12	−470[f]	210	−56
66	$D_2O + 1/3O/Pt(111) \rightarrow 2/3(D_2O\cdots OD)/Pt(111)$	1/2	−57	150	−507
67	$HCOOH + O/Pt(111) \rightarrow HCOO_{mon}/Pt(111) + OH/Pt(111)$	1/4	−78[f]	130	−345
68	$HCOOH + O/Pt(111) \rightarrow HCOO_{bi}/Pt(111) + OH/Pt(111)$	1/4	−113[f]	170	−381
69	$C_2H_4 + Ni(100) \rightarrow 2{\equiv}CH/Ni(100) + 2H/Ni(100)$	init.	−203	300	−57
70	$C_2H_4 + Ni(100) \rightarrow -CCH/Ni(100) + 3H/Ni(100)$	0.07	−140	300	53
71	$C_2H_4 + Ni(110) \rightarrow -CCH/Ni(110) + H/Ni(110)$	init.	−120	300	73
72	$C_2H_2 + Ni(100) \rightarrow 2{\equiv}CH/Ni(100)$	init.	−265	300	−19
73	$C_2H_2 + Ni(100) \rightarrow -CCH/Ni(100) + H/Ni(100)$	1/4	−150	300	124
74	$C_2H_2 + Ni(110) \rightarrow -CCH/Ni(110) + H/Ni(110)$	init.	−180	300	94
75	$C_2H_2 + Rh(100) \rightarrow -CCH/Rh(100) + H/Rh(100)$	init.	−175	300	87
76	$C_2H_4 + Pt(111) \rightarrow {=}CH{-}CH_3/Pt(111) + H/Pt(111)$	init.	−138	300	−50
77	$C_2H_4 + Pt(111) \rightarrow {\equiv}C{-}CH_3/Pt(111) + 1/2H_2$	1/6	−99	300	−47
78	$C_2H_4 + Pt(100)\text{-hex} \rightarrow {=}CH{-}CH{=}/Pt(100)\text{-hex} + 2H/Pt(100)\text{-hex}$	init.	−150	300	−25
79	$C_2H_4 + Pt(100)\text{-}(1\times1) \rightarrow {=}CH{-}CH{=}/Pt(100)\text{-}(1\times1) + 2H/Pt(100)\text{-}(1\times1)$	init.	−215	300	−90
80	$C_2H_4 + Pt(100)\text{-}(1\times1) \rightarrow -CH{=}CH{-}/Pt(100)\text{-}(1\times1) + 2H/Pt(100)\text{-}(1\times1)$	1/3	−106	300	19
81	$c\text{-}C_6H_{10} + Pt(111) \rightarrow c\text{-}C_6H_9/Pt(111) + H/Pt(111)$	0.12	−132[f]	281	−198

[a]Enthalpies of formation of gas-phase species were adjusted to the listed temperature using heat capacities of elements in their standard states and gas-phase heat capacities of relevant species (see Table S2). As heat capacities of adsorbed species are generally not known, we assumed that the heat capacity differences between adsorbates are negligible over the range of temperatures used. "Standard" here simply refers to 1 bar pressure and has no implications with respect to any specific coverage or temperature. [b]Enthalpies of formation correspond to the first adsorbate species on the right side of the reaction arrow, per mole of that adsorbate, *at the listed temperature and coverage* and 1 bar pressure for pure gas for all gases listed in the reaction. [c]Enthalpies of formation of adsorbates for systems 71, 73, 74, 76, and 77 were calculated as above but using enthalpies of formation of hydrogen on Ni(110), Rh(100), Pt(100)-(1 × 1), and Pt(100)-hex estimated based on the ΔH_f reported for adatoms on other crystal facets of the same metal since the value has not been reported for this facet to our knowledge. [d]These coverages are defined here as the number of reacted gas molecules in the reaction *as written* per metal surface atom, with the exception of reactions 27−45 where coverage refers to the number of adsorbed atoms per metal surface atom. [e]These are the enthalpy changes for the reaction per mole of reacted gas *as written*, integrated from zero coverage of the reacted gas up to its listed coverage. When necessary, enthalpy changes reported here are obtained from Arrhenius desorption barriers by subtracting $1/2RT$ from the positive barrier values and changing sign. [f]These entries were decreased in absolute magnitude by 2−3 kJ/mol from original publications, to correct a systematic error equal to RT_{source}, where T_{source} is the temperature of the molecular beam source (298−350 K). This arose due to a typographical error in ref 95, where a negative sign is missing in eqs (5) and (8) on "$1/2\ RT_{source}$."

on the above systems where multiple measurements are available, we estimate that values are accurate to within ±6 kJ/mol for the reactions *as written*. This is an important distinction, as errors for DFT are often given *per adsorbed fragment*.[18] For example, the estimated experimental error for the enthalpy of $O_2 + Pt(111) \rightarrow 2\ O/Pt(111)$ is 6 kJ/mol *as written*, but only 3 kJ/mol *per adsorbed fragment*.

Table 2 lists the experimental standard enthalpies of formation (ΔH^0_f) of the relevant adsorbed product, extracted from the reaction enthalpies listed in Table 1, along with the coverages and temperatures at which they were measured, and literature citations to the reaction enthalpies used from Table 1. For many adsorbates, these enthalpies of formation were determined from measurements of the heats of adsorption of gases on the clean metal surface that produce this single adsorbate, so they result from simply subtracting the standard enthalpy of formation of the gas molecule at the same temperature (determined from standard heats of formation and heat capacities of gas-phase species (see Table S2 for references and values used for gas species)) from the adsorption reaction's standard enthalpy of Table 1. For some adsorbates, however, the reactions whose experimental enthalpies are listed in Table 1 are not so simple, and so their enthalpies had to be combined with the standard heats of formation of both gas-phase species and other adsorbed species to get the heats of formation listed here. In doing this, we sometimes needed to assume that the heat capacity differences between adsorbates are negligible over the range of temperature differences used for this calculation,

DOI: 10.1021/acs.jpcc.6b06154
J. Phys. Chem. C 2016, 120, 25161−25172

due to the absence of any heat capacity data for adsorbates. Note that OH_{ad} is a common product listed here. It is likely that these OH_{ad} products disproportionate immediately upon production to make the $(H_2O{-}OH)_{ad}$ complex via the reaction $3OH_{ad} \rightarrow (H_2O{-}OH)_{ad} + O_{ad}$, but as this reaction is nearly thermoneutral, this would not affect this reaction's enthalpy nor any of the corresponding enthalpies of formation by more than 7 kJ/mol (or less, depending upon the coverage of O_{ad} produced). We list the reaction enthalpy here for the simpler reactions with OH_{ad} as the product, to simplify calculation of the enthalpies of formation. As the enthalpies of formation of $(H_2O{-}OH)_{ad}$ and O_{ad} are also listed in Table 2, the interested reader may recalculate values based on those products instead.

CONCLUSIONS

The energies of adsorbates containing H, N, C, O, and halogens that are of interest as intermediates, poisons, and promoters in catalytic reactions have been measured on well-defined single-crystal surfaces of numerous later transition metals by equilibrium adsorption isotherms, temperature-programmed desorption (TPD), and single-crystal adsorption calorimetry (SCAC). We have tabulated a large collection of those experimental adsorption energies which we consider to be particularly reliable based on reproducibility by other groups, comparisons to results for closely related systems, and/or reliability of other results reported by the same group. We have listed the enthalpies and energies of 81 molecular and dissociative adsorption reactions that were measured on 26 different metal single-crystal faces of 12 different late transition metals (Table 1), and we have extracted from these the standard enthalpies of formation of the 81 different adsorbates thus produced (Table 2).

ASSOCIATED CONTENT

Supporting Information

The Supporting Information is available free of charge on the ACS Publications website at DOI: 10.1021/acs.jpcc.6b06154.

Lists of enthalpies and energies of reactions used to calculate average values reported in Table 1 and enthalpies of formation and heat capacities of gas-phase species used in making Table 2 from the data in Table 1 (PDF)

AUTHOR INFORMATION

Corresponding Author

*E-mail: charliec@uw.edu. Tel.: 206-616-6085.

Notes

The authors declare no competing financial interest.

Biographies

Dr. Trent L. Silbaugh completed his thesis work in the laboratory of Professor Charles T. Campbell in the Chemical Engineering department at the University of Washington and is currently a postdoctoral researcher at the University of Michigan in the laboratory of Professor Mark A. Barteau. His research interests lie in gaining a deeper understanding of the fundamentals of heterogeneous catalytic processes through experimental studies of model catalyst systems. He received his BS (2009) from Arizona State University and his MS (2012) and PhD (2014) from the University of Washington.

Prof. Charles T. Campbell is the Rabinovitch Endowed Chair in Chemistry at the University of Washington, where he is also Adjunct Professor of Chemical Engineering and of Physics. He is the author of over 300 publications and two patents on surface chemistry, catalysis, physical chemistry and biosensing, with 18,000 total citations and an h-index of 72 (ISI Web of Science). He is an elected Fellow of both the ACS, the AVS and the AAAS, and Member of the Washington State Academy of Sciences. He received the Arthur W. Adamson Award of the ACS and the ACS Award for Colloid or Surface Chemistry, the Gerhard Ertl Lecture Award, the Robert Burwell Award/Lectureship of the North American Catalysis Society, the Medard W. Welch Award of the AVS, the Ipatieff Lectureship of Northwestern University, and an Alexander von Humboldt Research Award. He served as Editor-in-Chief of *Surface Science* for ten years and now serves as Editor-in-Chief of *Surface Science Reports* and on the Boards of the *Journal of Physical Chemistry*, *Catalysis Reviews*, *Catalysis Letters*, and *Topics in Catalysis*. He received his BS (1975) and PhD (1979) degrees at the University of Texas at Austin in Chemical Engineering and Chemistry, respectively, then did postdoctoral research in Germany under Gerhard Ertl (who won the 2007 Nobel Prize in Chemistry).

DOI: 10.1021/acs.jpcc.6b06154
J. Phys. Chem. C 2016, 120, 25161−25172

■ ACKNOWLEDGMENTS

Support for this work provided by the National Science Foundation under CHE-1361939.

■ REFERENCES

(1) Kresse, G.; Furthmuller, J. Efficiency of ab-initio total energy calculations for metals and semiconductors using a plane-wave basis set. *Comput. Mater. Sci.* **1996**, *6*, 15−50.
(2) Kresse, G.; Furthmuller, J. Efficient iterative schemes for ab initio total-energy calculations using a plane-wave basis set. *Phys. Rev. B: Condens. Matter Mater. Phys.* **1996**, *54*, 11169−11186.
(3) Hammer, B.; Hansen, L. B.; Norskov, J. K. Improved adsorption energetics within density-functional theory using revised Perdew-Burke-Ernzerhof functionals. *Phys. Rev. B: Condens. Matter Mater. Phys.* **1999**, *59*, 7413−7421.
(4) Segall, M. D.; Lindan, P. J. D.; Probert, M. J.; Pickard, C. J.; Hasnip, P. J.; Clark, S. J.; Payne, M. C. First-principles simulation: ideas, illustrations and the CASTEP code. *J. Phys.: Condens. Matter* **2002**, *14*, 2717−2744.
(5) Norskov, J. K.; Bligaard, T.; Kleis, J. Rate control and reaction engineering. *Science* **2009**, *324*, 1655−1656.
(6) Norskov, J. K.; Bligaard, T.; Rossmeisl, J.; Christensen, C. H. Towards the computational design of solid catalysts. *Nat. Chem.* **2009**, *1*, 37−46.
(7) Norskov, J. K.; Abild-Pedersen, F.; Studt, F.; Bligaard, T. Density functional theory in surface chemistry and catalysis. *Proc. Natl. Acad. Sci. U. S. A.* **2011**, *108*, 937−943.
(8) Besenbacher, F.; Chorkendorff, I.; Clausen, B. S.; Hammer, B.; Molenbroek, A. M.; Norskov, J. K.; Stensgaard, I. Design of a surface alloy catalyst for steam reforming. *Science* **1998**, *279*, 1913−1915.
(9) Studt, F.; Abild-Pedersen, F.; Bligaard, T.; Sorensen, R. Z.; Christensen, C. H.; Norskov, J. K. Identification of non-precious metal alloy catalysts for selective hydrogenation of acetylene. *Science* **2008**, *320*, 1320−1322.
(10) Mavrikakis, M. Computational methods: A search engine for catalysts. *Nat. Mater.* **2006**, *5*, 847−848.
(11) Nilekar, A. U.; Xu, Y.; Zhang, J. L.; Vukmirovic, M. B.; Sasaki, K.; Adzic, R. R.; Mavrikakis, M. Bimetallic and ternary alloys for improved oxygen reduction catalysis. *Top. Catal.* **2007**, *46*, 276−284.
(12) Alayoglu, S.; Nilekar, A. U.; Mavrikakis, M.; Eichhorn, B. Ru-Pt core-shell nanoparticles for preferential oxidation of carbon monoxide in hydrogen. *Nat. Mater.* **2008**, *7*, 333−338.
(13) Greeley, J.; Mavrikakis, M. Alloy catalysts designed from first principles. *Nat. Mater.* **2004**, *3*, 810−815.
(14) Greeley, J.; Jaramillo, T. F.; Bonde, J.; Chorkendorff, I. B.; Norskov, J. K. Computational high-throughput screening of electrocatalytic materials for hydrogen evolution. *Nat. Mater.* **2006**, *5*, 909−913.
(15) Greeley, J.; Norskov, J. K.; Kibler, L. A.; El-Aziz, A. M.; Kolb, D. M. Hydrogen evolution over bimetallic systems: Understanding the trends. *ChemPhysChem* **2006**, *7*, 1032−1035.
(16) Greeley, J.; Norskov, J. K. Large-scale, density functional theory-based screening of alloys for hydrogen evolution. *Surf. Sci.* **2007**, *601*, 1590−1598.
(17) Greeley, J.; Stephens, I. E. L.; Bondarenko, A. S.; Johansson, T. P.; Hansen, H. A.; Jaramillo, T. F.; Rossmeisl, J.; Chorkendorff, I.; Norskov, J. K. Alloys of platinum and early transition metals as oxygen reduction electrocatalysts. *Nat. Chem.* **2009**, *1*, 552−556.
(18) Wellendorff, J.; Silbaugh, T. L.; Garcia-Pintos, D.; Norskov, J. K.; Bligaard, T.; Studt, F.; Campbell, C. T. A benchmark database for adsorption bond energies to transition metal surfaces and comparison to selected DFT functionals. *Surf. Sci.* **2015**, *640*, 36−44.
(19) Gautier, S.; Steinmann, S. N.; Michel, C.; Fleurat-Lessard, P.; Sautet, P. Molecular adsorption at Pt(111). How accurate are DFT functionals? *Phys. Chem. Chem. Phys.* **2015**, *17*, 28921−28930.
(20) Campbell, C. T.; Sellers, J. R. V. Enthalpies and entropies of adsorption on well-defined oxide surfaces: Experimental measurements. *Chem. Rev.* **2013**, *113*, 4106−4135.
(21) Redhead, P. A. Chemisorption on polycrystalline tungsten 0.1. - carbon monoxide. *Trans. Faraday Soc.* **1961**, *57*, 641−656.
(22) Campbell, C. T.; Sellers, J. R. V. The entropies of adsorbed molecules. *J. Am. Chem. Soc.* **2012**, *134*, 18109−18115.
(23) Lord, F. M.; Kittelberger, Js determination of activation-energies in thermal desorption experiments. *Surf. Sci.* **1974**, *43*, 173−182.
(24) Falconer, J. L.; Madix, R. J. Flash desorption activation-energies - DCOOH decomposition and CO desorption from Ni(110). *Surf. Sci.* **1975**, *48*, 393−405.
(25) Habenschaden, E.; Kuppers, J. Evaluation of flash desorption spectra. *Surf. Sci.* **1984**, *138*, L147−L150.
(26) King, D. A.Thermal desorption from metal-surfaces. *Surf. Sci.* **1975**, *47*, 384−402.
(27) Dejong, A. M.; Niemantsverdriet, J. W. Thermal-desorption analysis - comparative test of 10 commonly applied procedures. *Surf. Sci.* **1990**, *233*, 355−365.
(28) Langmuir, I. The adsorption of gases on plane surfaces of glass, mica and platinum. *J. Am. Chem. Soc.* **1918**, *40*, 1361−1403.
(29) Tracy, J. C.; Palmberg, P. W. Structural influences on adsorbate binding energy.I. carbon monoxide on (100) palladium. *J. Chem. Phys.* **1969**, *51*, 4852.
(30) Christmann, K.; Ertl, G. Adsorption of carbon-monoxide on silver-palladium alloys. *Surf. Sci.* **1972**, *33*, 254.
(31) Engel, T.; Ertl, G. Molecular-beam investigation of catalytic-oxidation of CO on Pd(111). *J. Chem. Phys.* **1978**, *69*, 1267−1281.
(32) Wu, K. J.; Kevan, S. D. Isothermal coverage dependent measurements of NH3 and ND3 desorption from Cu(001). *J. Chem. Phys.* **1991**, *95*, 5355−5363.
(33) Peterson, L. D.; Kevan, S. D. Coverage-dependent desorption measurements for CO/Ag(011). *J. Chem. Phys.* **1991**, *95*, 8592−8598.
(34) Burghaus, U.; Conrad, H. A molecular-beam relaxation spectroscopy study of CO adsorption on Ag(110) and Pt(111). *Surf. Sci.* **1995**, *331*, 116−120.
(35) Brown, W. A.; Kose, R.; King, D. A. Femtomole adsorption calorimetry on single-crystal surfaces. *Chem. Rev.* **1998**, *98*, 797−831.
(36) Lytken, O.; Lew, W.; Campbell, C. T. Catalytic reaction energetics by single crystal adsorption calorimetry: hydrocarbons on Pt(111). *Chem. Soc. Rev.* **2008**, *37*, 2172−2179.
(37) Freund, H. J.; Nilius, N.; Risse, T.; Schauermann, S.; Schmidt, T. Innovative measurement techniques in surface science. *ChemPhysChem* **2011**, *12*, 79−87.
(38) Fischer-Wolfarth, J.-H.; Hartmann, J.; Farmer, J. A.; Flores-Camacho, J. M.; Campbell, C. T.; Schauermann, S.; Freund, H.-J. An improved single crystal adsorption calorimeter for determining gas adsorption and reaction energies on complex model catalysts. *Rev. Sci. Instrum.* **2011**, *82*, 024102.
(39) Karp, E. M.; Campbell, C. T.; Studt, F.; Abild-Pedersen, F.; Nerskov, J. K. Energetics of oxygen adatoms, hydroxyl species and water dissociation on Pt(111). *J. Phys. Chem. C* **2012**, *116*, 25772−25776.
(40) Lew, W. D.; Crowe, M. C.; Karp, E.; Campbell, C. T. Energy of molecularly adsorbed water on clean Pt(111) and Pt(111) with coadsorbed oxygen by calorimetry. *J. Phys. Chem. C* **2011**, *115*, 9164−9170.
(41) Lew, W.; Crowe, M. C.; Karp, E.; Lytken, O.; Farmer, J. A.; Arnadottir, L.; Schoenbaum, C.; Campbell, C. T. The Energy of Adsorbed Hydroxyl on Pt(111) by Microcalorimetry. *J. Phys. Chem. C* **2011**, *115*, 11586−11594.
(42) Columbia, M. R.; Crabtree, A. M.; Thiel, P. A. The temperature and coverage dependences of adsorbed formic-acid and its conversion to formate on Pt(111). *J. Am. Chem. Soc.* **1992**, *114*, 1231−1237.
(43) Baber, A. E.; Lawton, T. J.; Sykes, E. C. H. Hydrogen-bonded networks in surface-bound methanol. *J. Phys. Chem. C* **2011**, *115*, 9157−9163.
(44) Lawton, T. J.; Carrasco, J.; Baber, A. E.; Michaelides, A.; Sykes, E. C. H. Hydrogen-bonded assembly of methanol on Cu(111). *Phys. Chem. Chem. Phys.* **2012**, *14*, 11846−11852.

DOI: 10.1021/acs.jpcc.6b06154
J. Phys. Chem. C 2016, 120, 25161−25172

(45) Bishop, A. R.; Girolami, G. S.; Nuzzo, R. G. Structural models and thermal desorption energetics for multilayer assemblies of the n-alkanes on Pt(111). *J. Phys. Chem. B* **2000**, *104*, 754−763.
(46) Christmann, K. *Landolt-Boernstein, Group III*; Bonzel, H.-P., Ed.; Springer: 2006; Vol. *42*.
(47) Yeo, Y. Y.; Wartnaby, C. E.; King, D. A. Calorimetric measurement of the energy difference between 2 solid-surface phases. *Science* **1995**, *268*, 1731−1732.
(48) Christmann, K.; Schober, O.; Ertl, G. Adsorption of CO on a Ni(111) surface. *J. Chem. Phys.* **1974**, *60*, 4719−4724.
(49) Froitzheim, H.; Kohler, U. Kinetics of the adsorption of CO on Ni(111). *Surf. Sci.* **1987**, *188*, 70−86.
(50) Miller, J. B.; Siddiqui, H. R.; Gates, S. M.; Russell, J. N.; Yates, J. T.; Tully, J. C.; Cardillo, M. J. Extraction of kinetic-parameters in temperature programmed desorption - a comparison of methods. *J. Chem. Phys.* **1987**, *87*, 6725−6732.
(51) Skelton, D. C.; Wei, D. H.; Kevan, S. D. Interactions between adsorbed molecules: CO on Ni(111). *Surf. Sci.* **1997**, *370*, 64−70.
(52) Feigerle, C. S.; Desai, S. R.; Overbury, S. H. The kinetics of co desorption from Ni(110). *J. Chem. Phys.* **1990**, *93*, 787−794.
(53) Madden, H. H.; Kuppers, J.; Ertl, G. Interaction of carbon-monoxide with (110) nickel surfaces. *J. Chem. Phys.* **1973**, *58*, 3401−3410.
(54) Love, C. A.; Schultz, S. L.; Feigerle, C. S. A comparison of desorption rate parameters obtained by the variation of heating rate and the threshold temperature programmed desorption methods. *Surf. Sci.* **1991**, *244*, L143−L146.
(55) Tracy, J. C. Structural influences on adsorption energy 0.2. CO on Ni(100). *J. Chem. Phys.* **1972**, *56*, 2736.
(56) Benziger, J. B.; Madix, R. J. Decomposition of formic-acid on Ni(100). *Surf. Sci.* **1979**, *79*, 394−412.
(57) Labohm, F.; Engelen, C. W. R.; Gijzeman, O. L. J.; Geus, J. W.; Bootsma, G. A. Interaction of CO with Ni(100) - adsorption-isotherms and thermal-decomposition. *J. Chem. Soc., Faraday Trans. 1* **1982**, *78*, 2435−2446.
(58) Bordoli, R. S.; Vickerman, J. C.; Wolstenholme, J. Surface coverage measurements by SIMS for CO adsorption on a number of metals and for CO and H2S coadsorption on Ni(110), (100) and (111). *Surf. Sci.* **1979**, *85*, 244−262.
(59) Schiesser, A.; Hortz, P.; Schafer, R. Thermodynamics and kinetics of CO and benzene adsorption on Pt(111) studied with pulsed molecular beams and microcalorimetry. *Surf. Sci.* **2010**, *604*, 2098−2105.
(60) Campbell, C. T.; Ertl, G.; Kuipers, H.; Segner, J. A molecular-beam investigation of the interactions of CO with a Pt(111)surface. *Surf. Sci.* **1981**, *107*, 207−219.
(61) Kelemen, S. R.; Fischer, T. E.; Schwarz, J. A. Binding-energy of co on clean and sulfur covered platinum surfaces. *Surf. Sci.* **1979**, *81*, 440−450.
(62) Poelsema, B.; Palmer, R. L.; Comsa, G. A thermal he scattering study of CO adsorption on Pt(111). *Surf. Sci.* **1984**, *136*, 1−14.
(63) Jackman, T. E.; Davies, J. A.; Jackson, D. P.; Unertl, W. N.; Norton, P. R. The Pt(110) phase-transitions - a study by rutherford backscattering, nuclear microanalysis, leed and thermal-desorption spectroscopy. *Surf. Sci.* **1982**, *120*, 389−412.
(64) Fair, J.; Madix, R. J. Low and high coverage determinations of the rate of carbon-monoxide adsorption and desorption from Pt(110). *J. Chem. Phys.* **1980**, *73*, 3480−3485.
(65) Yeo, Y. Y.; Vattuone, L.; King, D. A. Energetics and kinetics of CO and NO adsorption on Pt{100}: Restructuring and lateral interactions. *J. Chem. Phys.* **1996**, *104*, 3810−3821.
(66) Ratajczykowa, I. The influence of CO on hydrogen sorption by Pd(111) single-crystals. *Surf. Sci.* **1986**, *172*, 691−714.
(67) Kok, G. A.; Noordermeer, A.; Nieuwenhuys, B. E. Decomposition of methanol and the interaction of coadsorbed hydrogen and carbon-monoxide on a Pd(111) surface. *Surf. Sci.* **1983**, *135*, 65−80.
(68) Conrad, H.; Ertl, G.; Koch, J.; Latta, E. E. Adsorption of CO on Pd single-crystal surfaces. *Surf. Sci.* **1974**, *43*, 462−480.
(69) Noordermeer, A.; Kok, G. A.; Nieuwenhuys, B. E. Comparison between the adsorption properties of Pd(111) and PdCu(111) surfaces for carbon-monoxide and hydrogen. *Surf. Sci.* **1986**, *172*, 349−362.
(70) Kiskinova, M. P.; Bliznakov, G. M. Adsorption and co-adsorption of carbon-monoxide and hydrogen on Pd(111). *Surf. Sci.* **1982**, *123*, 61−76.
(71) Guo, X. C.; Yates, J. T.Dependence of effective desorption kinetic-parameters on surface coverage and adsorption temperature - CO on Pd(111). *J. Chem. Phys.* **1989**, *90*, 6761−6766.
(72) Behm, R. J.; Christmann, K.; Ertl, G.; Vanhove, M. A. Adsorption of CO on Pd(100). *J. Chem. Phys.* **1980**, *73*, 2984−2995.
(73) Szanyi, J.; Goodman, D. W. CO oxidation on palladium 0.1. a combined kinetic-infrared reflection-absorption spectroscopic study of Pd(100). *J. Phys. Chem.* **1994**, *98*, 2972−2977.
(74) Wei, D. H.; Skelton, D. C.; Kevan, S. D. Desorption and molecular interactions on surfaces: CO/Rh(110), CO/Rh(100) and CO/Rh(111). *Surf. Sci.* **1997**, *381*, 49−64.
(75) Peterlinz, K. A.; Curtiss, T. J.; Sibener, S. J. Coverage dependent desorption-kinetics of CO from Rh(111) using time-resolved specular helium scattering. *J. Chem. Phys.* **1991**, *95*, 6972−6985.
(76) Seebauer, E. G.; Kong, A. C. F.; Schmidt, L. D. Adsorption and desorption of CO and H-2 on Rh(111) - laser-induced desorption. *Appl. Surf. Sci.* **1988**, *31*, 163−172.
(77) Sushchikh, M.; Lauterbach, J.; Weinberg, W. H. Chemisorption of CO on the Ir(111) surface: Adsorption and desorption kinetics measured with in situ vibrational spectroscopy. *J. Vac. Sci. Technol., A* **1997**, *15*, 1630−1634.
(78) Hinch, B. J.; Dubois, L. H. 1st-order corrections in modulated molecular-beam desorption experiments. *Chem. Phys. Lett.* **1990**, *171*, 131−135.
(79) Hollins, P.; Pritchard, J. Interactions of CO molecules adsorbed on Cu(111). *Surf. Sci.* **1979**, *89*, 486−495.
(80) Pfnur, H.; Feulner, P.; Engelhardt, H. A.; Menzel, D. Example of fast desorption - anomalously high pre-exponentials for CO desorption from Ru(001). *Chem. Phys. Lett.* **1978**, *59*, 481−486.
(81) Vickerman, J. C.; Christmann, K.; Ertl, G. Model studies on bimetallic Cu-Ru catalysts 0.3. adsorption of carbon-monoxide. *J. Catal.* **1981**, *71*, 175−191.
(82) Lahtinen, J.; Vaari, J.; Kauraala, K. Adsorption and structure dependent desorption of CO on Co(0001). *Surf. Sci.* **1998**, *418*, 502−510.
(83) McElhiney, G.; Papp, H.; Pritchard, J. Adsorption of Xe and CO on Ag(111). *Surf. Sci.* **1976**, *54*, 617−634.
(84) Gottfried, J. M.; Schmidt, K. J.; Schroeder, S. L. M.; Christmann, K. Adsorption of carbon monoxide on Au(110)-(1 × 2). *Surf. Sci.* **2003**, *536*, 206−224.
(85) Fiorin, V.; Borthwick, D.; King, D. A. Microcalorimetry of O2 and NO on flat and stepped platinum surfaces. *Surf. Sci.* **2009**, *603*, 1360−1364.
(86) Wartnaby, C. E.; Stuck, A.; Yeo, Y. Y.; King, D. A. Microcalorimetric heats of adsorption for CO, NO, and oxygen on Pt(110). *J. Phys. Chem.* **1996**, *100*, 12483−12488.
(87) Ramsier, R. D.; Gao, Q.; Waltenburg, H. N.; Lee, K. W.; Nooij, O. W.; Lefferts, L.; Yates, J. T. NO adsorption and thermal-behavior on Pd surfaces - a detailed comparative-study. *Surf. Sci.* **1994**, *320*, 209−237.
(88) Ge, Q. F.; Kose, R.; King, D. A. Adsorption energetics and bonding from femtomole calorimetry and from first principles theory. *Adv. Catal.* **2000**, *45*, 207−259.
(89) Parker, D. H.; Bartram, M. E.; Koel, B. E. Study of high coverages of atomic oxygen on the Pt(111) surface. *Surf. Sci.* **1989**, *217*, 489−510.
(90) Campbell, C. T.; Ertl, G.; Kuipers, H.; Segner, J. A molecular-beam study of the adsorption and desorption of oxygen from a Pt(111) surface. *Surf. Sci.* **1981**, *107*, 220−236.
(91) Bozso, F.; Ertl, G.; Grunze, M.; Weiss, M. Interaction of nitrogen with iron surfaces 0.1. Fe(100) and Fe(111). *J. Catal.* **1977**, *49*, 18−41.

DOI: 10.1021/acs.jpcc.6b06154
J. Phys. Chem. C 2016, 120, 25161−25172

(92) Conrad, H.; Ertl, G.; Kuppers, J.; Latta, E. E. Adsorption of CO on clean and oxygen covered Ni(111) surfaces. *Surf. Sci.* **1976**, *57*, 475−484.
(93) Gardin, D. E.; Batteas, J. D.; Vanhove, M. A.; Somorjai, G. A. Carbon, nitrogen, and sulfur on Ni(111) - formation of complex structures and consequences for molecular decomposition. *Surf. Sci.* **1993**, *296*, 25−35.
(94) Poelsema, B.; Lenz, K.; Comsa, G. The dissociative adsorption of hydrogen on Pt(111): Actuation and acceleration by atomic defects. *J. Chem. Phys.* **2011**, *134*, 074703.
(95) Lytken, O.; Lew, W.; Harris, J. J. W.; Vestergaard, E. K.; Gottfried, J. M.; Campbell, C. T. Energetics of cyclohexene adsorption and reaction on Pt(111) by low-temperature microcalorimetry. *J. Am. Chem. Soc.* **2008**, *130*, 10247−10257.
(96) Christmann, K. Interaction of hydrogen with solid-surfaces. *Surf. Sci. Rep.* **1988**, *9*, 1−163.
(97) Bozso, F.; Ertl, G.; Grunze, M.; Weiss, M. Chemisorption of hydrogen on iron surfaces. *Appl. Surf. Sci.* **1977**, *1*, 103−119.
(98) Yates, J. T.; Thiel, P. A.; Weinberg, W. H. Chemisorption of hydrogen on Rh(111). *Surf. Sci.* **1979**, *84*, 427−439.
(99) Engstrom, J. R.; Tsai, W.; Weinberg, W. H. The chemisorption of hydrogen on the (111) and (110)-(1 × 2) surfaces of iridium and platinum. *J. Chem. Phys.* **1987**, *87*, 3104−3119.
(100) Feulner, P.; Menzel, D. The adsorption of hydrogen on ruthenium (001) - adsorption states, dipole-moments and kinetics of adsorption and desorption. *Surf. Sci.* **1985**, *154*, 465−488.
(101) Smith, A. H.; Barker, R. A.; Estrup, P. J. Desorption of hydrogen from tungsten (100). *Surf. Sci.* **1984**, *136*, 327−344.
(102) Labayen, M.; Furman, S. A.; Harrington, D. A. A thermal desorption study of iodine on Pt(111). *Surf. Sci.* **2003**, *525*, 149−158.
(103) Schennach, R.; Bechtold, E. Chlorine adsorption on Pt(111) and Pt(110). *Surf. Sci.* **1997**, *380*, 9−16.
(104) Bechtold, E. Adsorption of fluorine on Pt(111). *Appl. Surf. Sci.* **1981**, *7*, 231−240.
(105) Karp, E. M.; Silbaugh, T. L.; Campbell, C. T. Energetics of adsorbed CH3 and CH on Pt(111) by calorimetry: Dissociative adsorption of CH3I. *J. Phys. Chem. C* **2013**, *117*, 6325−6336.
(106) Karp, E. M.; Silbaugh, T. L.; Crowe, M. C.; Campbell, C. T. Energetics of adsorbed methanol and methoxy on Pt(111) by microcalorimetry. *J. Am. Chem. Soc.* **2012**, *134*, 20388−20395.
(107) Silbaugh, T. L.; Karp, E. M.; Campbell, C. T. Energetics of formic acid conversion to adsorbed formates on Pt(111) by transient calorimetry. *J. Am. Chem. Soc.* **2014**, *136*, 3964−3971.
(108) Tait, S. L.; Dohnalek, Z.; Campbell, C. T.; Kay, B. D. n-alkanes on Pt(111) and on C(0001)/Pt(111): Chain length dependence of kinetic desorption parameters. *J. Chem. Phys.* **2006**, *125*, 234308.
(109) Ihm, H.; Ajo, H. M.; Gottfried, J. M.; Bera, P.; Campbell, C. T. Calorimetric measurement of the heat of adsorption of benzene on Pt(111). *J. Phys. Chem. B* **2004**, *108*, 14627−14633.
(110) Xi, M.; Yang, M. X.; Jo, S. K.; Bent, B. E.; Stevens, P. Benzene adsorption on Cu(111) - formation of a stable bilayer. *J. Chem. Phys.* **1994**, *101*, 9122−9131.
(111) Lukas, S.; Vollmer, S.; Witte, G.; Woll, C. Adsorption of acenes on flat and vicinal Cu(111) surfaces: Step induced formation of lateral order. *J. Chem. Phys.* **2001**, *114*, 10123−10130.
(112) Zhou, X. L.; Castro, M. E.; White, J. M. Interactions of uv photons and low-energy electrons with chemisorbed benzene on Ag(111). *Surf. Sci.* **1990**, *238*, 215−225.
(113) Syomin, D.; Kim, J.; Koel, B. E.; Ellison, G. B. Identification of adsorbed phenyl (C6H5) groups on metal surfaces: Electron-induced dissociation of benzene on Au(111). *J. Phys. Chem. B* **2001**, *105*, 8387−8394.
(114) Gottfried, J. M.; Vestergaard, E. K.; Bera, P.; Campbell, C. T. Heat of adsorption of naphthalene on Pt(111) measured by adsorption calorimetry. *J. Phys. Chem. B* **2006**, *110*, 17539−17545.
(115) Karp, E. M.; Silbaugh, T. L.; Campbell, C. T. Energetics of adsorbed CH3 on Pt(111) by calorimetry. *J. Am. Chem. Soc.* **2013**, *135*, 5208−5211.
(116) Wolcott, C. A.; Green, I. X.; Silbaugh, T. L.; Xu, Y.; Campbell, C. T. Energetics of adsorbed CH2 and CH on Pt(111) by calorimetry: The dissociative adsorption of diiodomethane. *J. Phys. Chem. C* **2014**, *118*, 29310−29321.
(117) Liu, W.; Maaß, F.; Willenbockel, M.; Bronner, C.; Schulze, M.; Soubatch, S.; Tautz, F. S.; Tegeder, P.; Tkatchenko, A. Quantative pridction of molecular adsorption: Structure and binding of Benzene on coinage metals. *Phys. Rev. Lett.* **2015**, *115*, 036104.

DOI: 10.1021/acs.jpcc.6b06154
J. Phys. Chem. C 2016, 120, 25161−25172